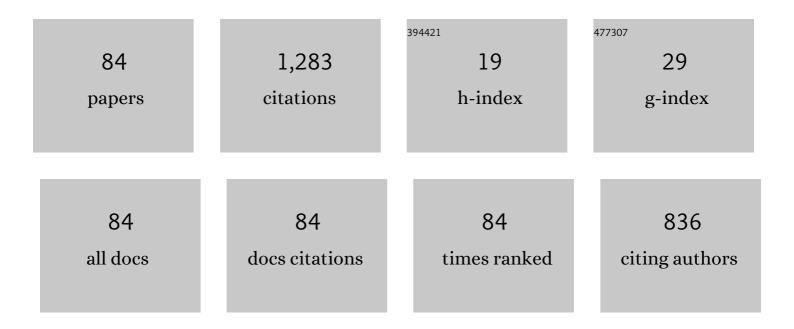
List of Publications by Year in descending order

Source: https://exaly.com/author-pdf/2858437/publications.pdf Version: 2024-02-01



#	Article	IF	CITATIONS
1	Scintillation characteristics of Nd ³⁺ -doped BaO–Al ₂ O ₃ –TeO ₂ glasses. Japanese Journal of Applied Physics, 2022, 61, SB1034.	1.5	3
2	Preparation and scintillation properties of the Eu3+-activated SrO–Al2O3–TeO2 glasses. Materials Research Bulletin, 2022, 145, 111547.	5.2	20
3	Optical, scintillation and thermoluminescent properties of Eu2O3-doped K2O–La2O3–Ga2O3 glasses. Radiation Physics and Chemistry, 2022, 190, 109785.	2.8	11
4	Formation of highly dispersed tin nanoparticles in amorphous silicates for sodium ion battery anode. Journal of Physics and Chemistry of Solids, 2022, 161, 110377.	4.0	7
5	Fracture toughness enhancement via subâ€micro silverâ€precipitation in silica glass fabricated by spark plasma sintering. Journal of the American Ceramic Society, 2022, 105, 1980-1991.	3.8	6
6	In Situ Growth Mechanism of CsPbX ₃ (X = Cl, Br, and I) Quantum Dots in an Amorphous Oxide Matrix. Chemistry of Materials, 2022, 34, 1599-1610.	6.7	12
7	Radiation Response Characteristics of Pr3+-activated SrO–Al2O3–TeO2 Glasses. Sensors and Materials, 2022, 34, 707.	0.5	9
8	Development of Photo-functional Glasses with Nanostructure Induced though Bond Selectivity in Oxyfluoride. Funtai Oyobi Fummatsu Yakin/Journal of the Japan Society of Powder and Powder Metallurgy, 2022, 69, 68-72.	0.2	0
9	Ultrafast Nanocrystallization of BaF ₂ in Oxyfluoride Glasses with Crystal-like Nanostructures: Implications for Upconversion Fiber Devices. ACS Applied Nano Materials, 2022, 5, 4281-4292.	5.0	3
10	Radiation response properties of Eu3+-doped K2O–Ta2O5–Ga2O3 glasses. Ceramics International, 2022, 48, 9353-9361.	4.8	8
11	Scintillation characteristics of Eu2O3-doped WO3–Al2O3–TeO2 glasses. Journal of Luminescence, 2022, 249, 119003.	3.1	8
12	Microstructure and improved fracture toughness of borosilicate glass reinforced by 1 vol% Ag nanoparticles. Ceramics International, 2022, 48, 30900-30904.	4.8	4
13	Aluminum for Near Infrared Plasmonics: Amplified Upâ€Conversion Photoluminescence from Core–Shell Nanoparticles on Periodic Lattices. Advanced Optical Materials, 2021, 9, .	7.3	27
14	Synthesis of Luminescent Eu(III)-Doped Octacalcium Phosphate Particles Hybridized with Succinate Ions and Their Reactive Behavior in Simulated Body Fluid. Crystal Growth and Design, 2021, 21, 2005-2018.	3.0	4
15	Up-conversion Luminescence Enhanced by the Plasmonic Lattice Resonating at the Transparent Window of Water. ACS Applied Energy Materials, 2021, 4, 2999-3007.	5.1	14
16	Optical and radiation response characteristics of Eu2O3-doped K2O–Bi2O3–Ga2O3 glasses. Ceramics International, 2021, 47, 11596-11601.	4.8	12
17	Toughening silica glass by imparting ductility using a small amount of silver nanoparticles. Materials Science & Engineering A: Structural Materials: Properties, Microstructure and Processing, 2021, 817, 141372.	5.6	14
18	Interfacial heterogeneous precipitation of Ag nanoparticles in soda-lime silicate glass for improved toughness and conductivity. Ceramics International, 2021, 47, 24466-24475.	4.8	5

#	Article	IF	CITATIONS
19	Near-infrared engineering for broad-band wavelength-tunable in biological window of NIR-â; and -â¢: A solid solution phosphor of Sr1-xCaxTiO3:Ni2+. Journal of Luminescence, 2021, 238, 118235.	3.1	38
20	Utility of Tissue Classification in Invasive Ductal Carcinoma using Dynamic Magnetic Resonance Imaging of the Mammary Gland. Journal of Clinical Imaging Science, 2021, 11, 4.	1.1	0
21	Scintillation and TSL properties of Nd-doped TeO2–Al2O3-WO3 glasses. Solid State Sciences, 2020, 100, 106111.	3.2	17
22	Improvement in microstructure and thermo-mechanical properties of MgO-based dry vibratable material by addition of Fe. Materials Chemistry and Physics, 2020, 253, 123368.	4.0	7
23	Impact of crystallization method on the strain, defect formation, and thermoluminescence of YAG:Ce crystals. Journal of Alloys and Compounds, 2020, 849, 156600.	5.5	7
24	Structural origin of high-density Gd2O3–MoO3–B2O3 glass and low-density β′-Gd2(MoO4)3 crystal: a study conducted using high-energy x-ray diffraction and EXAFS at high temperatures. Journal of Physics Condensed Matter, 2020, 32, 055705.	1.8	4
25	Scintillation properties of organic–inorganic layered perovskite nanocrystals in glass. Journal of Applied Physics, 2020, 127, .	2.5	16
26	Massive red shift of Ce ³⁺ in Y ₃ Al ₅ O ₁₂ incorporating super-high content of Ce. RSC Advances, 2020, 10, 12535-12546.	3.6	32
27	Photoluminescence and scintillation properties of Al(PO3)3–CeCl3–CsCl–CsPO3 glass scintillators. Journal of Materials Science: Materials in Electronics, 2020, 31, 4488-4493.	2.2	16
28	Rapid Synthesis of Quantum-Sized Organic–Inorganic Perovskite Nanocrystals in Glass. Scientific Reports, 2020, 10, 1237.	3.3	9
29	Structural study of WO3-La2O3-B2O3-Nb2O5 glasses. Journal of Non-Crystalline Solids, 2020, 543, 120132.	3.1	20
30	Scintillation properties of Dy-doped TeO ₂ –Al ₂ O ₃ –BaO glasses. Journal of the Ceramic Society of Japan, 2020, 128, 1024-1029.	1.1	11
31	Plasmonic Enhancement of Upconversion Photoluminescence from CaF ₂ : Er ³⁺ , Yb ³⁺ Nanoparticles on TiN Nanoantennas. Funtai Oyobi Fummatsu Yakin/Journal of the Japan Society of Powder and Powder Metallurgy, 2020, 67, 140-145.	0.2	2
32	Enhanced growth of Y3al5O12:Ce3+ nanocrystals in mesoporous SiO2 utilizing vacuum-assisted impregnation. Processing and Application of Ceramics, 2020, 14, 141-145.	0.8	0
33	Photoluminescence and structural similarity of crystals with oxide–fluoride stacking structure and oxyfluoride glass. Journal of the Ceramic Society of Japan, 2020, 128, 1030-1037.	1.1	6
34	Effect of Mg ²⁺ and fluorine on the network and highly efficient photoluminescence of Eu ³⁺ ion in MgF ₂ –BaO–B ₂ O ₃ glasses. Journal of the American Ceramic Society, 2019, 102, 2531-2541.	3.8	9
35	Radio-photoluminescence observed in Eu-doped BABF glass-ceramics. Ceramics International, 2019, 45, 9376-9380.	4.8	19
36	Phase-Selective Distribution of Eu ²⁺ and Eu ³⁺ in Oxide and Fluoride Crystals in Glass-Ceramics for Warm White-Light-Emitting Diodes. ACS Applied Electronic Materials, 2019, 1, 961-971.	4.3	61

#	Article	IF	CITATIONS
37	Scintillator and dosimeter properties of Ce3+ doped CaF2AlF3AlPO4 glasses. Optical Materials, 2019, 94, 86-91.	3.6	15
38	Photoluminescence and scintillation properties of Eu-doped TeO2-Al2O3-BaO glasses. Journal of Materials Science: Materials in Electronics, 2019, 30, 11468-11474.	2.2	12
39	X-ray induced luminescence properties of Ce-doped BaF2-Al2O3-B2O3 glasses. Optical Materials, 2019, 90, 64-69.	3.6	18
40	Photo-, radio- and thermo- luminescence properties of Eu-doped BaSi2O5 glass-ceramics. Optik, 2019, 185, 812-818.	2.9	9
41	Dosimetric, luminescence and scintillation properties of Ce-doped CaF2-Al2O3-B2O3 glasses. Journal of Non-Crystalline Solids, 2019, 509, 60-64.	3.1	14
42	Scintillation properties of Ce-doped SrF2-Al2O3-B2O3 glasses. Journal of Non-Crystalline Solids, 2019, 508, 46-50.	3.1	30
43	Synthesis of new transparent borate-based BaF2 nanocrystallized glass by formation of nucleation sites induced by rare earth ions. Journal of the European Ceramic Society, 2019, 39, 1735-1739.	5.7	15
44	Tb3+-doped BaF2-Al2O3-B2O3 glass and glass-ceramic for radiation measurements. Journal of Non-Crystalline Solids, 2018, 501, 111-115.	3.1	17
45	Characterizations of Pr-doped Yb3Al5O12 single crystals for scintillator applications. Solid State Sciences, 2018, 78, 1-6.	3.2	11
46	Simultaneous surface and bulk crystallization of Bi _{1.5} ZnNb _{1.5} O ₇ â€type pyrochlores and related crystals in glasses. International Journal of Applied Glass Science, 2018, 9, 296-304.	2.0	4
47	Control of self-powdering phenomenon in ferroelastic β′-Gd2(MoO4)3 crystallization in boro-tellurite glasses. Journal of Non-Crystalline Solids, 2018, 501, 85-92.	3.1	4
48	Luminescence of Ce 3+ in aluminophosphate glasses prepared in air. Journal of Luminescence, 2018, 195, 413-419.	3.1	21
49	Design of crystallization of oxyfluoride glasses based on the local structure of fluorine. Journal of the Ceramic Society of Japan, 2018, 126, 684-692.	1.1	4
50	Scintillation and VUV-excited photoluminescence of europium-doped BaF2–Al2O3–B2O3 glasses. Journal of Materials Science: Materials in Electronics, 2018, 29, 11824-11829.	2.2	14
51	Preparation of calcium phosphate nanoparticles hybridized with europium(III) complex for novel luminescent organic-inorganic systems. Journal of Physics and Chemistry of Solids, 2018, 122, 218-226.	4.0	11
52	Nano-crystallization and highly oriented crystal line patterning of Sm3+-doped Bi2GeO5 and Bi4Ge3O12 in bismuth germanate-based glasses. Journal of Non-Crystalline Solids, 2017, 459, 116-122.	3.1	12
53	Radio-photoluminescence in Sm-doped BaF2-Al2O3-B2O3 glass-ceramics. Radiation Measurements, 2017, 106, 73-78.	1.4	37
54	Highly efficient red-emitting BaMgBO3F:Eu3+,R+(R: Li, Na, K, Rb) phosphor for near-UV excitation synthesized via glass precursor solid-state reaction. Japanese Journal of Applied Physics, 2017, 56, 092601.	1.5	6

#	Article	IF	CITATIONS
55	Enhancement of photoluminescence of glass phosphor by nanoimprint of moth-eye structure. Journal of the Ceramic Society of Japan, 2017, 125, 766-769.	1.1	1
56	A Simple Incorporation Route of Tris(8-hydroxyquinoline)aluminum(III) into Transparent Mesoporous Silica Films and Their Photofunctions. Hindawi Journal of Chemistry, 2017, 2017, 1-10.	1.6	3
57	Optical and magneto-optical properties of Bi substituted yttrium iron garnets prepared by metal organic decomposition. Optical Materials Express, 2016, 6, 1986.	3.0	43
58	Dielectric properties of glass-ceramics with Ba1â^'xY2x/3Nb2O6 nanocrystals and laser patterning of highly oriented crystal lines. Journal of Non-Crystalline Solids, 2016, 452, 74-81.	3.1	7
59	Unique thermal conductivity, Young's modulus and local structure of 72SnO–28P ₂ O ₅ glass. Journal of the Ceramic Society of Japan, 2016, 124, 606-612.	1.1	8
60	Long afterglow in hexagonal SrAl2O4:Eu2+, Dy3+ synthesized by crystallization of glass and solidification of supercooled melts. Journal of Luminescence, 2016, 177, 286-289.	3.1	15
61	Electrochemical performance as cathode of lithium iron silicate, borate and phosphate glasses with different Fe2+ fractions. Journal of Non-Crystalline Solids, 2016, 436, 51-57.	3.1	13
62	TEM analysis for crystal structure of metastable BiBO3 (II) phase formed in glass by laser-induced crystallization. Journal of the European Ceramic Society, 2015, 35, 2541-2546.	5.7	15
63	Laser Patterning of Non-Linear Optical Bi2ZnB2O7 Crystal Lines in Glass. Frontiers in Materials, 2015, 2,	2.4	9
64	Self-organized homo-epitaxial growth in nonlinear optical BaAlBO3F2 crystal crossing lines patterned by laser in glass. Optical Materials, 2015, 49, 182-189.	3.6	11
65	Structure of MoO3–WO3–La2O3–B2O3 glasses and crystallization of LaMo1â^'xWxBO6 solid solutions. Journal of Non-Crystalline Solids, 2015, 429, 171-177.	3.1	17
66	Glass structure and NIR emission of Er3+ at 1.5 μm in oxyfluoride BaF2–Al2O3–B2O3 glasses. Optical Materials, 2015, 50, 238-243.	3.6	29
67	Morphology and orientation of β-BaB2O4 crystals patterned by laser in the inside of samarium barium borium borate glass. Journal of Solid State Chemistry, 2015, 221, 145-151.	2.9	20
68	Electrical conductivity of Na2O–Nb2O5–P2O5 glass and fabrication of glass–ceramic composites with NASICON type Na3Zr2Si2PO12. Solid State Ionics, 2015, 269, 19-23.	2.7	53
69	Electronic polarizability and interaction parameter of gadolinium tungsten borate glasses with high WO3 content. Journal of Solid State Chemistry, 2014, 220, 191-197.	2.9	25
70	Synthesis and photocatalytic properties of α-ZnWO4 nanocrystals in tungsten zinc borate glasses. Journal of Asian Ceramic Societies, 2014, 2, 253-257.	2.3	17
71	Crystallization behavior of sodium iron phosphate glass Na2â^'Fe1+0.5P2O7 for sodium ion batteries. Journal of Non-Crystalline Solids, 2014, 404, 26-31.	3.1	53
72	High quantum yield and low concentration quenching of Eu3+ emission in oxyfluoride glass with high BaF2 and Al2O3 contents. Optical Materials, 2014, 36, 1384-1389.	3.6	41

#	Article	IF	CITATIONS
73	Coexistence of nano-scale phase separation and micro-scale surface crystallization in Gd2O3–WO3–B2O3 glasses. Journal of Non-Crystalline Solids, 2013, 381, 17-22.	3.1	14
74	Morphology and photoluminescence properties of Er3+-doped CaF2 nanocrystals patterned by laser irradiation in oxyfluoride glasses. Journal of Fluorine Chemistry, 2013, 145, 81-87.	1.7	28
75	Effect of AlN addition on spatial uniform distribution of Er ³⁺ -doped CaF ₂ nanocrystals in oxyfluoride glass-ceramics. Journal of the Ceramic Society of Japan, 2013, 121, 457-459.	1.1	6
76	Synthesis and morphology of Ba1â^'RE2/3Nb2O6 nanocrystals with tungsten bronze structure in RE2O3–BaO–Nb2O5–B2O3 glasses (RE: Sm, Eu, Gd, Dy, Er). Journal of Solid State Chemistry, 2012, 196, 384-390.	2.9	17
77	Morphology and dispersion state of Ba2TiSi2O8 nanocrystals in transparent glass-ceramics and their nanoindentation behavior. Journal of Non-Crystalline Solids, 2012, 358, 1863-1869.	3.1	22
78	New oxyfluoride glass with high fluorine content and laser patterning of nonlinear optical BaAlBO3F2 single crystal line. Journal of Applied Physics, 2012, 112, .	2.5	31
79	Fluorine deficient layer at the surface of transparent glass-ceramics with CaF2 nanocrystals. Journal of Physics and Chemistry of Solids, 2012, 73, 683-687.	4.0	19
80	Nanoindentation Analysis of Elastic/Mechanical Behaviour of Surface of Transparent Glass Ceramics with Fresnoite Ba2TiSi2O8Nanocrystals. IOP Conference Series: Materials Science and Engineering, 2011, 21, 012020.	0.6	1
81	Elastic properties and Vickers hardness of optically transparent glass–ceramics with fresnoite Ba2TiSi2O8 nanocrystals. Materials Research Bulletin, 2011, 46, 922-928.	5.2	27
82	Morphology of CaF2 nanocrystals and elastic properties in transparent oxyfluoride crystallized glasses. Optical Materials, 2011, 33, 1350-1356.	3.6	41
83	Thermal conductivity and mechanical properties of soda-lime glass with interfacially connected Au layer fabricated via sputtering and spark plasma sintering. Journal of Asian Ceramic Societies, 0, , 1-6.	2.3	0
84	Selfâ€6training Nanocrystals Strategy: Temperature and Pressure Coâ€Induced Phase Transitions of CsPbBr ₃ in Amorphous Matrices. Advanced Optical Materials, 0, , 2200818.	7.3	2